OFFICE OF NAVAL RESEARCH

Research Contract N00014-90-J-1178

R&T Code 413r008---001

Principal Investigator: **R. Stanley Williams**
Organization: **Regents of the University of California**

TECHNICAL REPORT No. 10

SUBMICRON-SCALE SURACE ROUGHENING INDUCED BY ION BOMBARDMENT

by

E.A. Eklund, R. Bruinsma, J. Rudnick and R. Stanley Williams

Submitted to

Physical Review Letters

University of California, Los Angeles
Department of Chemistry & Biochemistry and Solid State Sciences Center
Los Angeles, CA 90024-1569

February, 1991

UNCLASSIFIED

SECURITY CLASSIFICATION OF THIS PAGE

REPORT DOCUMENTATION PAGE

1a REPORT SECURITY CLASSIFICATION UNCLASSIFIED	1b RESTRICTIVE MARKINGS N/A
2a SECURITY CLASSIFICATION AUTHORITY N/A	3 DISTRIBUTION/AVAILABILITY OF REPORT Approved for public release; distribution unlimited
2b DECLASSIFICATION/DOWNGRADING SCHEDULE N/A	
4 PERFORMING ORGANIZATION REPORT NUMBER(S) N/A	5 MONITORING ORGANIZATION REPORT NUMBER(S)
6a NAME OF PERFORMING ORGANIZATION The Regents of the University of California 6b OFFICE SYMBOL (If applicable)	7a NAME OF MONITORING ORGANIZATION 1) ONR Pasadena - Administrative 2) ONR Alexandria - Technical
6c ADDRESS (City, State, and ZIP Code) Office of Contracts & Grants Administration U C L A, 405 Hilgard Avenue Los Angeles, CA 90024	7b ADDRESS (City, State, and ZIP Code) 1) 1030 E. Green Street, Pasadena, CA 91106 2) 800 N. Quincy St., Arlington, VA 22217-500
8a NAME OF FUNDING/SPONSORING ORGANIZATION Office of Naval Research 8b OFFICE SYMBOL (If applicable) ONR	9 PROCUREMENT INSTRUMENT IDENTIFICATION NUMBER N00014-90-J-1178
8c ADDRESS (City, State, and ZIP Code) 800 N. Quincy Street, 614A:DHP Arlington, VA 22217-5000	10 SOURCE OF FUNDING NUMBERS PROGRAM ELEMENT NO / PROJECT NO / TASK NO / WORK UNIT ACCESSION NO

11 TITLE (Include Security Classification)

UNCLASSIFIED: SUBMICRON-SCALE SURACE ROUGHENING INDUCED BY ION BOMBARDMENT

12 PERSONAL AUTHOR(S) **E.A. Eklund, R. Bruinsma, J. Rudnick and R. Stanley Williams**

13a TYPE OF REPORT	13b TIME COVERED	14 DATE OF REPORT (Year, Month, Day)	15 PAGE COUNT
Tech.Rpt.#10	FROM June'90 TO Feb'91	91/2/28	8 pp 4 Figs

16 SUPPLEMENTARY NOTATION

17 COSATI CODES		
FIELD	GROUP	SUB-GROUP

18 SUBJECT TERMS (Continue on reverse if necessary and identify by block number)

scanning tunneling microscope - sputter etching - graphite bombarded by argon - surface morphology - correlation length vs ion dose

19 ABSTRACT (Continue on reverse if necessary and identify by block number)

The scanning tunneling microscope (STM) was used to quantitatively investigate sputter etching of graphite surfaces bombarded by 5 keV argon ions. The resulting surface morphology depended strongly on ion flux, dose and sample temperature. The height-height correlation functions of the roughened surfaces were calculated directly from the STM topographs and were compared to linear response theory and scaling analyses for the propagation of growing fronts. We find that the surfaces develop structures characterized by a correlation length that diverges with increasing ion dose.

20 DISTRIBUTION/AVAILABILITY OF ABSTRACT ☒ UNCLASSIFIED/UNLIMITED ☐ SAME AS RPT ☐ DTIC USERS	21 ABSTRACT SECURITY CLASSIFICATION UNCLASSIFIED
22a NAME OF RESPONSIBLE INDIVIDUAL R. Stanley Williams	22b TELEPHONE (Include Area Code) (213) 825-8818 22c OFFICE SYMBOL UCLA

DD FORM 1473, 84 MAR 83 APR edition may be used until exhausted
All other editions are obsolete

SECURITY CLASSIFICATION OF THIS PAGE

UNCLASSIFIED

Sub-micron Scale Surface Roughening Induced by Ion Bombardment

Elliott A. Eklund, R. Bruinsma and J. Rudnick

Department of Physics

University of California, Los Angeles CA 90024-1547

and

R. Stanley Williams

Department of Chemistry & Biochemistry

University of California, Los Angeles CA 90024-1569

ABSTRACT

The scanning tunneling microscope (STM) was used to quantitatively investigate sputter etching of graphite surfaces bombarded by 5 keV argon ions. The resulting surface morphology depended strongly on ion flux, dose and sample temperature. The height-height correlation functions of the roughened surfaces were calculated directly from the STM topographs and were compared to linear response theory and scaling analyses for the propagation of growing fronts. We find that the surfaces develop structures characterized by a correlation length that diverges with increasing ion dose.

PACS numbers: 68.55.Jk, 79.20.Rf, 81.15.Cd

One of the fundamental challenges in materials science is to understand the effects of particle radiation on solid surfaces.[1-3] For example, the properties of sputter-deposited thin films depend strongly on the surface topology, which in turn is determined by the sputter-growth process.[4] Ion-beam sputter etching, a widely used technique in surface science and microelectronics, also produces surfaces with characteristic morphologies that depend on the sputtering conditions.

On the macroscopic level (*i.e.*, length scales larger than one micron), the effects of particle radiation on surfaces are well understood. Ion bombardment erodes edges, corners and peaks preferentially because prominent features are exposed to a larger flux. This smoothing of surface roughness is further enhanced by diffusion and evaporation/recondensation. In the continuum description of this process, one either assumes that the local erosion rates are proportional to the local incoming flux, or one uses the so-called "Huyghens Construction."[5] Numerical studies of macroscopic evolution have obtained results that compare favorably with experiments.[6,7]

At the sub-micron level, our understanding is much less complete.[8] Electron-microscope studies indicate that particle radiation *roughens* a surface, and prominent cone-like features have been reported.[9,10] Both analytical studies and Monte Carlo simulations[11,12] of the effect of shot noise on continuum theories indicate that stochastic processes roughen surfaces. The roughening is characterized by a correlation length $\xi(t)$ that diverges with etching time t. Until now, however, there has been little experimental confirmation of this description.

In this Letter, we report on our use of a Scanning Tunneling Microscope (STM)[13] to study the surface topography of graphite after sputter etching. The STM offers unique opportunities for the study of radiation erosion because, unlike

the electron microscope, it can *quantitatively* measure the height profile h(r) of the surface over a wide range of length scales. This allows us to calculate the height-height correlation function[14] $\langle |h(q)|^2 \rangle$, defined as:

$$\langle |h(q)|^2 \rangle = \int \frac{d^2r}{(2\pi)^2} e^{iq.r} \langle (h(o) - h(r))^2 \rangle_t / \text{Area}, \quad (1)$$

with $\langle \cdots \rangle_t$ indicating a sample average after t seconds of exposure. In other roughening problems, *e.g.*, thermal roughening, the corresponding correlation function is a good measure of the overall surface geometry.[15] Because of loss of phase information in the height-height correlation function, however, it is less sensitive to uncorrelated -- but prominent -- surface features, which are much more easily visible in the real space STM topographs.

The surface chosen for this investigation was the cleaved (0001) face of highly oriented pyrolytic graphite (HOPG). This surface is inert in air and is easily imaged with the STM.[13] Graphite also has a rigid lattice, with a melting temperature of ~3800°C. This indicates that surface diffusion should be minimal at room temperature and thus bombardment induced topography is "frozen in" and can be observed with the STM long after sputtering has occurred.

Freshly cleaved graphite samples were examined with the STM before sputter etching. The microscope was operated at atmospheric pressure in the constant current mode, with a tunnel current of 0.5 nA and a sample to tip bias of -100 mV. No filtering or data enhancement was necessary because of the especially high stability of our STM with respect to vibrational, electrical and thermal disturbances. Low magnification topographs (2400 Å x 2400 Å image size) showed large, atomically flat areas over many thousands of square Ångstroms,

while at higher magnifications (25 Å x 25 Å) the familiar atomic scale features of clean graphite were easily observed.[13]

After stable images of clean graphite were obtained, the samples were transferred to the sample treatment chamber of a KRATOS XSAM-800 surface analytical system. The graphite surfaces were sputter etched with a beam of 5 keV Ar^+ ions, rastered over a 9 mm^2 area on the sample and incident at an angle of 60° to the surface normal. The beam flux incident on the sample was determined by using an electrometer to measure the ion beam current. A small positive bias (45 volts) was applied to the sample to suppress secondary electron emission. The experimental parameters that were varied in this study were the flux J, the ion dose Q = Jt, and the substrate temperature T.

This Letter highlights the results obtained from over 1,000 STM topographs collected from more than 15 bombarded samples. The two fluxes reported here are 6.9×10^{13} ions/cm^2 sec and 3.5×10^{14} ions/cm^2 sec. By varying the time of exposure to the ion beam, the total doses obtained were 10^{16}, 10^{17} and 10^{18} ions/cm^2. In addition to the ambient temperature experiments, etching was also performed at surface temperatures of approximately 600K and 900K for a flux of 3.5×10^{14} ions/cm^2 sec and a dose of 10^{17} ions/cm^2.

The graphite samples were re-examined with the STM after etching using identical operating parameters and, if possible, the same tunneling tip used prior to sputtering. The results shown in this study were reproducible from sample to sample and even with different tunneling tips, demonstrating that tip artifacts were minimal. Topographs with obvious imaging artifacts were observed, but were discarded. Figs. 1 - 3 show 2400Å x 2400Å images of sputtered graphite for the three different ion doses. The sample was etched at the lower flux. The corresponding correlation functions are shown in Fig. 4a. The sample average $\langle |h(q)|^2 \rangle$ of the two-dimensional Fourier transform power spectrum was obtained

by performing a rotational average of $|h(q)|^2$, sampling at increments of 1° for each value of q. The variance of $\langle |h(q)|^2 \rangle$ was also calculated to provide an estimate of the uncertainty in the correlation function.

The surface topology depended strongly on the ion dose. If we define the corrugation as the slope of a line connecting two surface points separated laterally by a distance L, Fig. 1 shows that this quantity becomes small for L larger than the correlation length, $\xi \approx 100 - 200$Å. Thus, for such length scales, the surface can be considered to be flat. As the dose Q increases (Figs. 2 & 3), ξ increases as well, and at the highest doses ξ exceeds the image size. For this real space behavior, one would expect that the correlation function should be q-independent for $q \lesssim 1/\xi$, while it should decrease with q for $q \gtrsim 1/\xi$, as observed in Fig. 4a.

The creation of correlated structures by particle radiation is counter-intuitive. However, theoretical studies of the non-equilibrium growth of interfaces[11,12] indicate that correlation resulting from random events is possible. A linear response theory was proposed for radiation erosion in ref. 16 and we now test its predictions by comparing the asymptotic limits to the experimental data. In linear response theory:

$$\partial_t h(\mathbf{q},t) = -\omega(\mathbf{q})\, h(\mathbf{q},t) + \eta(\mathbf{q},t) , \qquad (2)$$

where $\omega(\mathbf{q})$ is the healing rate of a surface modulation of wavevector $\mathbf{q}$ and $\eta(\mathbf{q},t)$ is the Gaussian white noise for the incident ions with a variance proportional to the flux J. For the case of isotropic radiation erosion including annealing by surface diffusion, the healing rate $\omega(\mathbf{q}) \propto J|\mathbf{q}| + D|\mathbf{q}|^4$, with D proportional to the surface diffusion constant. The resulting correlation function is :

$$\langle |h(\mathbf{q})|^2 \rangle_t \propto \frac{J}{\omega(\mathbf{q})} \left[1 - \exp(-2\omega(\mathbf{q})t)\right] . \qquad (3)$$

According to Eq.(3), for small q, $\langle |h(q)|^2 \rangle_t$ is proportional to t and independent of q, while for large q it decreases with q, indicating two distinct regions in plots of $\langle |h(q)|^2 \rangle_t$ vs. q. Fig. 4a shows that this type of behavior is observed experimentally. The transition should occur at the crossover wavevector $q_o = \xi^{-1}$, defined by $\omega(\xi^{-1})\, t = 1$, which predicts that the correlation length at crossover, $\xi \propto Q = Jt$ (assuming $\xi \lesssim (D/J)^{1/3}$). From Fig. 4a, we see that ξ increases with dose Q, albeit more slowly than linearly. In Fig. 4b, we show $\langle |h(q)|^2 \rangle_t$ for the same three doses as for Fig. 4a, but with J increased by a factor of 5. Indeed, within the uncertainties of the experimental data, ξ does not appear to have changed significantly for surfaces sputtered with the higher flux, even though these surfaces were rougher, ie. had larger values of $\langle |h(q)|^2 \rangle_t$.

We also investigated the behavior of Eq.(3) for elevated temperatures. For large q, $\omega(q) \propto Dq^4$, *so that* $\lim_{q \to \infty} \langle |h(q)|^2 \rangle_t \propto J/(Dq^4)$. This q^{-4} tail should be more pronounced at elevated temperatures, since D increases rapidly with T. In Fig. 4c, we show the T-dependence of $\langle |h(q)|^2 \rangle$ at the values of J and Q of Fig. 2. Above 600°K, $\langle |h(q)|^2 \rangle$ drops more sharply with q and, for large q, has a tail with an approximately q^{-4} dependence. For lower T, we found no q^{-4} tail down to 0.1 $Å^{-1}$ in any of our topographs.

By expanding the exponential term in Eq.(3) for the limit $q \to 0$, we see that the interface width, $W \equiv \lim_{q \to 0} \langle |h(q)|^2 \rangle_t^{1/2}$, should be proportional to $(Jt)^{1/2} = Q^{1/2}$, a prediction which is *independent* of our choice of the healing rate function, $\omega(q)$. For large doses (ie. long times) and $q > 0$, the exponential term is small and can be neglected, making $\langle |h(q)|^2 \rangle_t$ independent of the dose Q. From the experimental results in Figs. 4a and 4b, we see that W increases more like Q than $Q^{1/2}$ and that $\langle |h(q)|^2 \rangle_t$ shows a significant dose dependence at large q. Thus, although linear

response theory qualitatively accounts for a number of the observed features, it does not provide us with a quantitative description of our data.

At present, no non-linear theory exists for radiation erosion, but a general scaling description[12] has been developed in the context of various growth models.[11] According to scaling theory:

$$\langle |h(q)|^2 \rangle_t \propto q^{-\nu} F(t\, q^z), \tag{4}$$

with $F(x) \propto x^{\nu/z}$ for small x, and F(x) ~ constant for large x. This would predict a power law decrease, $q^{-\nu}$, in $\langle |h(q)|^2 \rangle_t$ for $q \gtrsim t^{-1/z}$. In Fig. 4a, we see an approximate power law dependence in the correlation function at large q for the *lower* ion doses, with an associated exponent of order -2.5 to -2.9. Under conditions of rotational invariance, the exponent z is related to ν by $z = 2 - \alpha$, with $2\alpha = \nu - 2$, resulting in z ~ 1.6 - 1.8 and ν/z ~ 1.5. This would mean that for small q, $\langle |h(q)|^2 \rangle_t \sim t^{\nu/z}$ should increase *faster* than linearly with increasing time (dose), while the correlation length at crossover, $\xi \sim t^{1/z}$, should increase *more slowly* than linearly. As we have seen, both predictions are valid for the experiments in this study. The values of α obtained from numerical studies in three dimensions are model dependent:[17] for weak non-linearity, α ~ 0.15 - 0.23 while α is ~ 4.0 for strong coupling. For our experiments, we find α to be ~ 0.2 - 0.4. The results embodied in Fig. 4 thus appear to be consistent with local growth models, at least at lower doses. We find this agreement somewhat surprising, as there is no *a priori* reason to expect a local growth model to correctly describe erosion via sputtering.[16]

In summary, ion bombarded graphite surfaces evolve a rough morphology characterized by the divergence of the correlation length, as predicted by linear response theory. However, the experimental height-height correlation function is

not quantitatively consistent with a linear response argument, but does have features in common with the scaling theory for sputter growth.

This work was supported by the National Science Foundation through Grant DMR 8922027 and by the Office of Naval Research. We would like to thank L. Golubovic and R.P.U. Karunasiri for helpful discussions and E. Snyder for assistance with the computer software.

References

1. J. L. Vossen and W. Kern, *Thin-Film Processes* (Academic Press, New York: 1978)
2. H. J. Mathieu, in *Thin Film and Depth Profile Analysis,* H. Oeschner, ed. (Springer-Verlag, Berlin: 1984), pp. 39-58.
3. G. Carter, in *Erosion and Growth of Solids Stimulated by Atom and Ion Beams,* G. Kiriakidis, G. Carter, and J. L. Whitton, eds. (Martinus Nijhoff, Hingham, MA: 1986), pp. 70-97.
4. I. J. Hodginson and P. W. Wilson, CRC Reviews **15,** 27 (1988).
5. See, for example, G. Carter and M. J. Nobes, Earth Surface Processes **5,** 131 (1980).
6. I. V. Katardjiev, J. Vac. Sci. Technol. **A 6** (4), 2434 (1988).
7. J. A. Kubby and B. M. Siegel, in *Erosion and Growth of Solids Stimulated by Atom and Ion Beams,* G. Kiriakidis, G. Carter, and J. L. Whitton, eds. (Martinus Nijhoff, Hingham, MA: 1986), pp. 444-452.
8. See, for example, D. M. Mattox, J. Vac. Sci. Technol. **A 7,** 1105 (1989).
9. G. Carter, B. Navinsek, and J. L. Whitton, in *Sputtering by Particle Bombardment, Vol. II,* R. Behrisch, ed. (Springer-Verlag, Berlin: 1983), pp. 231-266.
10. G. K. Wehner, J. Vac. Sci. Technol. **A 3,** 1821 (1985).
11. M. Kardar, G. Parisi and Y. C. Zhang, Phys. Rev. Lett. **56,** 889 (1986). For a review, see T. Vicsek, *Fractal Growth Phenomena* (World Scientific, Singapore, 1989).
12. F. Family and T. Vicsek, J. Phys. **A 18,** L75 (1985).
13. P.K. Hansma and J. Tersoff, J. Appl. Phys. **61** (2), R1 (1987).

14. For earlier measurements of $\langle |h(q)|^2 \rangle$ by microscopy, see G. Rasigni *et. al.*, Surface Science **162**, 985 (1985).

15. J. D. Weeks, in *Ordering in Strongly Fluctuating Condensed Matter Systems* (Plenum, New York, 1980), pp. 293.

16. G. S. Bales, *et al.*, Science **249**, 264 (1990).

17. H. Yan, D. Kessler and L. M. Sander, Phys. Rev. Lett. **64**, 926 (1990).

Figure Captions

Fig. 1 Constant current STM topograph of a graphite surface after sputtering with a flux J of 6.9×10^{13} ions/cm^2 sec and an ion dose Q of 10^{16} ions/cm^2 at room temperature. The X and Y dimensions are 2400 Å and the total Z dimension is 18.6 Å.

Fig. 2 STM topograph with the same parameters as that in Fig. 1, except that Q = 10^{17} ions/cm^2 and the total Z scale is 27.9 Å.

Fig. 3 STM topograph with the same parameters as that in Fig. 1, except that Q = 10^{18} ions/cm^2 and the total Z scale is 231.5 Å.

Fig. 4 Height-height correlation functions:

(a) $\langle |h(q)|^2 \rangle$ for the data in Figs. 1-3, with Q = 10^{16} ions/cm^2 (○), 10^{17} ions/cm^2 (■), and 10^{18} ions/cm^2 (◇). The crossover wavevector $q_o = 1/\xi$ is indicated for each curve and a $1/q^{2.7}$ dependence is shown for comparison in the large q regime. The error bars indicate one standard deviation in $\langle |h(q)|^2 \rangle$. The uncertainty decreases as q increases and at large q the error bars are within the size of the symbols for the data points.

(b) $\langle |h(q)|^2 \rangle$ for topographs with the same parameters as in Fig. 4a, except that the flux is higher: J = 3.5×10^{14} ions/cm^2 sec. Note that there is a significant flux dependence, with $\langle |h(q)|^2 \rangle$ larger (the surfaces are rougher) for the higher flux.

(c) Temperature dependence of $\langle |h(q)|^2 \rangle$ with J = 3.5×10^{14} ions/cm^2-sec, Q = 10^{17} ions/cm^2 and T = 300K (□), T = 600K (●) and T = 900K (♦). A $1/q^4$ dependence is shown for comparison in the large q regime. Note that $\langle |h(q)|^2 \rangle$ decreases (the surfaces are smoother) with increasing T.

FIG. 1

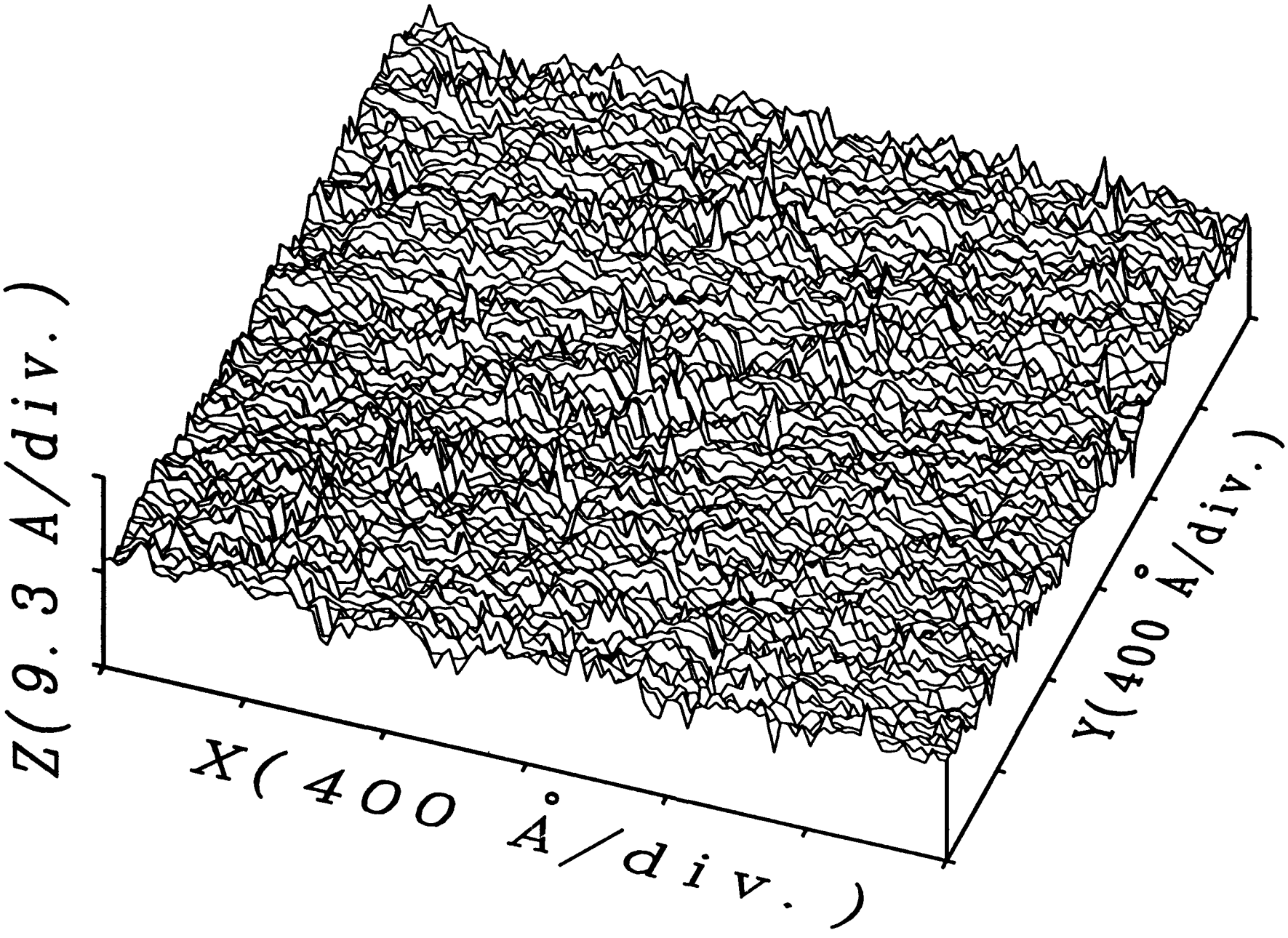

FIG. 2

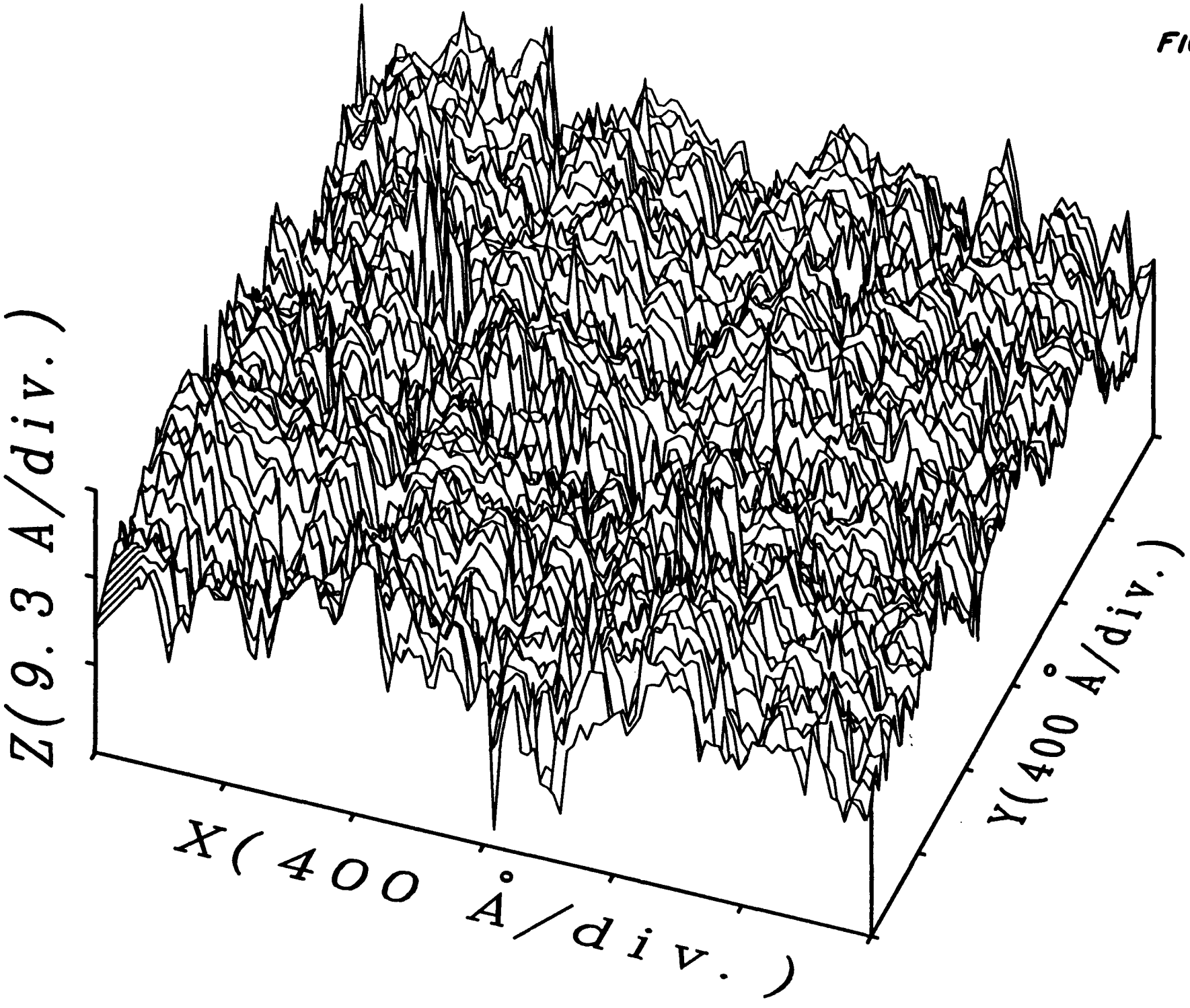

FIG. 3

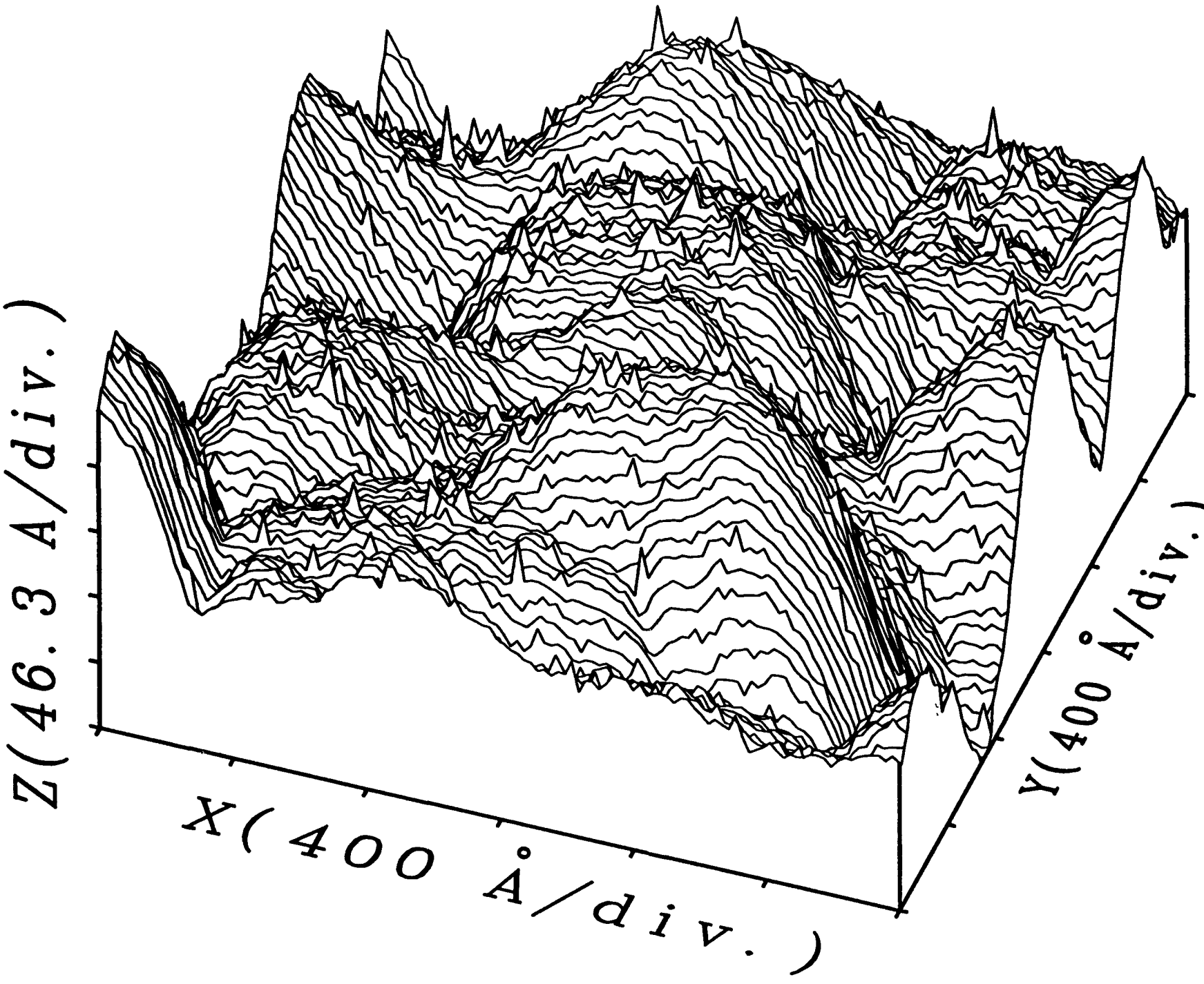

Fig. 4